

Article

Subsidence Evolution of the Leizhou Peninsula, China, Based on InSAR Observation from 1992 to 2010

Yanan Du ^{1,2}, Guangcai Feng ^{1,2,*}, Xing Peng ^{1,2} and Zhiwei Li ^{1,2}

Table S1. The parameters of the ascending ALOS-1 images selected.

Track	Frame	Acquisition Time	Perpendicular Baseline	Incident Angle(°)	Track	Frame	Acquisition time	Perpendicular Baseline	Incident Angle(°)
466	400	20070305	-62	38.75	467	390, 400, 410	20061220	-1005	38.75
466	400	20070905	512	38.75	467	390, 400, 410	20070204	-550	38.76
466	400	20080121	928	38.75	467	390, 400, 410	20070807	-49	38.75
466	400	20080723	-384	38.74	467	390, 400, 410	20071223	0	38.76
466	400	20090310	-644	38.75	467	390, 400, 410	20080207	648	38.76
466	400	20090910	-289	38.75	467	390, 400, 410	20081225	-1613	38.75
466	400	20091211	0	38.75	467	390, 400, 410	20090209	-1135	38.75
466	400	20100313	802	38.75	467	390, 400, 410	20090627	-696	38.76
466	400	20100729	954	38.75	467	390, 400, 410	20091228	-215	38.75
					467	390, 400, 410	20100212	207	38.76
					467	390, 400, 410	20100630	400	38.76

Note: Red italic bold represents SAR images which are contaminated by serious atmosphere. 20100126 of track466/frame400 is deleted due to the disagreement of new methods' rules, namely the identified image should be treated as master and slave in turn for the final used differential pairs.

Table S2. The parameters of the descending JERS images selected.

Path	Row	Acquisition time	Perpendicular baseline	Incident angle(°)
111	265/266	19921019	340	38.64
111	265/266	19940923	-1014	38.69
111	265/266	19950501	-1676	38.66
111	265/266	19950728	-564	38.81
111	265/266	19960304	1264	38.84
111	265/266	19970219	0	38.51
111	265/266	19970404	2260	38.83
111	265/266	19980322	-681	39.31
111	265/266	19980505	1624	39.06
111	265/266	19980801	2287	39.18
111	265/266	19980914	-622	39.34

Note: Red italic bold represents SAR images which are contaminated by serious atmosphere. 19931119 of path111/row265, 266 are deleted due to the failure of Modular SAR Processor (MSP) processing of GAMMA software.

Table S3. The parameters of the descending ENVISAT images selected.

Track	Acquisition time	Perpendicular baseline	Incident Angle(°)	Track	Acquisition time	Perpendicular baseline	Incident angle(°)	Track	Acquisition time	Perpendicular baseline	Incident Angle(°)
21	20031127	310	22.82	261	20031108	-997	22.82	261	20031108	-978	22.82
21	20040101	1072	22.84	261	20040327	849	22.83	261	20041023	664	22.83
21	20040415	759	22.84	261	<i>20041023</i>	642	22.83	261	20050101	-151	22.82
21	<i>20040624</i>	0	22.83	261	<i>20050101</i>	-149	22.82	261	<i>20050312</i>	0	22.83
21	20041216	-76	22.83	261	<i>20050312</i>	0	22.83	261	20050625	386	22.82
21	20050224	-129	22.82	261	20050625	375	22.82	261	<i>20060121</i>	-1187	22.82
21	<i>20050818</i>	230	22.83	261	20060121	-1200	22.83	261	20060610	-455	22.84
21	20070510	224	22.85	261	20060610	-468	22.84	261			

Note: Red italic bold represents SAR images which are contaminated by serious atmosphere. 20031023, 20041111 of track21 are deleted due to the disagreement of new methods' rules; 20040205 and 20050714 of track21 are deleted due to the failure of MSP processing.

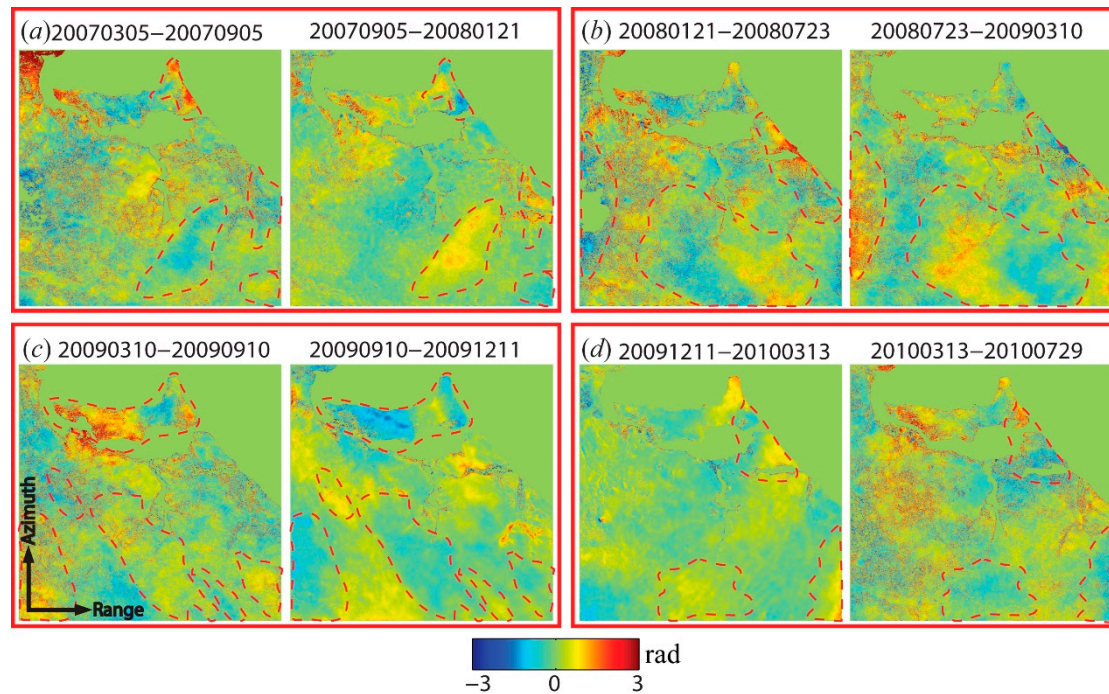


Figure S1. The atmospheric phase of ALOS1, track466 and frame400 in SAR coordination. The coverage of these images is represented by a black rectangle on the right-hand side in Figure 1. The wrapped phase of the differential interferogram whose master and slave images are the same SAR image with serious atmospheric delay. For example, 20070905, 20080723, 20090910 and 2010313 for (a–d) respectively. The red dashed lines in (a–d) represent the obvious atmospheric delay of each SAR image.

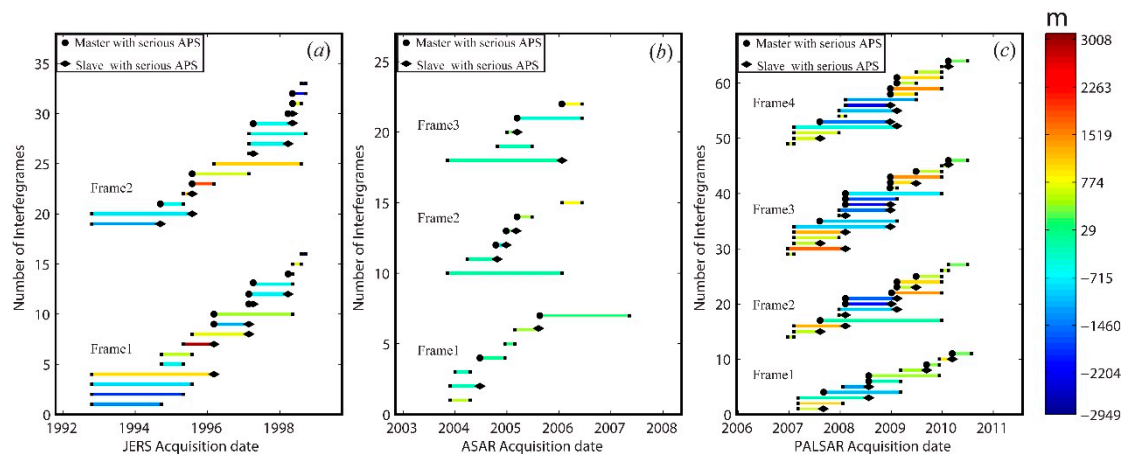


Figure S2. Perpendicular baselines and temporal intervals of the selected InSAR image pairs from three different sensors, JERS (a), ENVISAT (b) and ALOS-1 (c). The black dots and diamond represent SAR image contaminated with serious atmospheric delay used as a master and a slave, respectively.

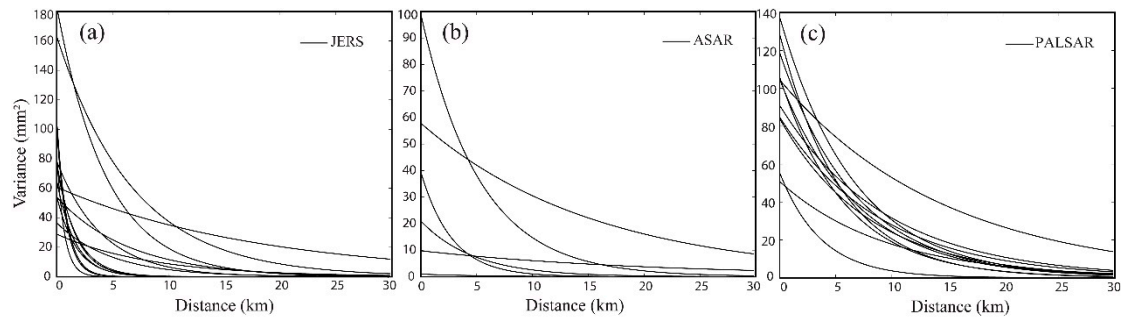


Figure S3. 1-D exponential covariance function of residual errors between the estimated displacement phase, calculated by the multiplication between velocity and time, and the single differential interferometric phase for each platform. The primary component in residual errors is caused by atmosphere, which can be estimated with 1-D exponential covariance function. **a–c** Show statistical results of the frame covered Zhanjiang city with JERS, ENVISAT and ALOS1, respectively. Every black curve in **(a–c)** represents a statistical result of residual error for a selected pair.